

Article

Diurnal to Seasonal Variations in Ocean Chlorophyll and Ocean Currents in the North of Taiwan Observed by Geostationary Ocean Color Imager and Coastal Radar

Po-Chun Hsu ^{1,2} , Ching-Yuan Lu ¹, Tai-Wen Hsu ²  and Chung-Ru Ho ^{1,*} 

¹ Department of Marine Environmental Informatics, National Taiwan Ocean University, Keelung 20224, Taiwan; hpochun@mail.ntou.edu.tw (P.-C.H.); 20681002@ntou.edu.tw (C.-Y.L.)

² Center of Excellence for Ocean Engineering, National Taiwan Ocean University, Keelung 20224, Taiwan; twhsu@mail.ntou.edu.tw

* Correspondence: b0211@mail.ntou.edu.tw

Received: 6 August 2020; Accepted: 31 August 2020; Published: 2 September 2020



Abstract: The waters in the north of Taiwan are located at the southern end of the East China Sea (ECS), adjacent to the Taiwan Strait (TS), and the Kuroshio region. To understand the physical dynamic process of ocean currents and the temporal and spatial distribution of the ocean chlorophyll concentration in the north of Taiwan, hourly coastal ocean dynamics applications radar (CODAR) flow field data and geostationary ocean color imager (GOCI) data are analyzed here. According to data from December 2014 to May 2020, the water in the TS flows along the northern coast of Taiwan into the Kuroshio region with a velocity of 0.13 m/s in spring and summer through the ECS. In winter, the Kuroshio invades the ECS shelf, where the water flows into the TS through the ECS with a velocity of 0.08 m/s. The seasonal variation of ocean chlorophyll concentration along the northwestern coast of Taiwan is obvious, where the average chlorophyll concentration from November to January exceeds 2.0 mg/m³, and the lowest concentration in spring is 1.4 mg/m³. It is apparent that the tidal currents in the north of Taiwan flow eastward and westward during ebb and flood periods, respectively. Affected by the background currents, the flow velocity exhibits significant seasonal changes, namely, 0.43 m/s in summer and 0.27 m/s in winter during the ebb period and is 0.26 m/s in summer and 0.45 m/s in winter during the flood period. The chlorophyll concentration near the shore is also significantly affected by the tidal currents. Based on CODAR data, virtual drifter experiments, and GOCI data, this research provides novel and important knowledge of ocean current movement process in the north of Taiwan and indicates diurnal to seasonal variations in the ocean chlorophyll concentration, facilitating future research on the interaction between the TS, ECS, and Kuroshio.

Keywords: GOCI; ocean chlorophyll concentration; coastal radar; drifter; tidal currents

1. Introduction

1.1. Background

The waters in the north of Taiwan are located at the southern end of the East China Sea (ECS). The Taiwan Strait (TS) is on the west and the Kuroshio is on the east (Figure 1). The Kuroshio branch, the South China Sea (SCS) surface current, and the China Coastal Current change seasonally in the TS [1–3]. Affected by changes in water masses, zooplankton clusters could vary with the seasons of ocean currents, with obviously temporal and spatial changes [4,5]. When the Kuroshio flows through the edge of the continental shelf, it may fully mix a large amount of coastal water.

With suitable water temperature and sufficient nutrient supply, ocean environments could trigger vigorous photosynthesis and rise primary productivity, which would provide abundant food for marine life in order to multiply rapidly and in large numbers, thus forming important fishing grounds [6,7]. The concentration of ocean chlorophyll could reflect the amount of phytoplankton, which is the lowest link in the marine food chain. The photosynthesis of phytoplankton would form the ocean's primary productivity. Therefore, the concentration of chlorophyll in the ocean could be regarded as one of the most critical indicators of the ocean's primary productivity. Analyzing the distribution of chlorophyll concentration in the north of Taiwan could help to understand the distribution of biological resources and habitats [8]. To study the continuous change of the chlorophyll concentration and the movement of ocean currents, geostationary ocean color imager (GOCI) data analysis is the best choice. With continuous observations during the daytime and cloud free, this could provide monthly and long-term period data, besides analyzing short-term diurnal changes. The GOCI data, with a high spatial resolution of 500 m, are conducive to the observation of nearshore hydrological changes, and these data have been successfully used to study submesoscale turbulence [9], biochemical monitoring in a bay [10], and mesoscale eddies [11].

Except for the cold dome in the north of Taiwan [12], breakthrough research has only begun in recent years because of the complicated flow conditions. In previous results, researchers have used satellite altimeter data and hydrological analysis methods to point out that there is a coastal regurgitation from the northeastern coast of Taiwan to the I-Lan Bay in the opposite direction to the Kuroshio. The source of this could be the cold dome or it could come from the ECS shelf. Based on the hydrological analysis data of ship surveys, the water in the I-Lan Bay has the characteristics of the ECS shelf water and the nearshore water of the Kuroshio [13]. Following this study, the researchers used in situ observations of ocean currents at specific locations to confirm that cyclonic eddies in the northeast of Taiwan could cause countercurrents [14], also found that the Kuroshio invasion could also produce coastal countercurrents [15]. However, these studies have pointed out that due to the lack of continuous ocean current observations, it is impossible to judge the dynamic process of water exchange. It is difficult to continuously measure ocean currents in coastal waters with traditional observation surveys and satellite observations. Using the coastal ocean dynamics applications radar (CODAR) data from Taiwan's ocean radar observing system (TOROS) [16], researchers have successfully observed sub-mesoscale ocean physical processes between the coral habitat and tidal currents in the southern bay of Taiwan [17]. Therefore, CODAR data is an appropriate way to observe continuous ocean currents.

1.2. Objectives

At present, the dynamic process and chlorophyll concentration changes in different months and seasons in the north of Taiwan are still unclear because the flow field situation is complicated and frequently changes. In this study, we first analyze the data of shipboard acoustic Doppler current profilers (Sb-ADCP) from over the past 30 years, then we use real drifter cases to present the continuity of the movement of water in the north of Taiwan. After roughly recognizing the characteristics of the flow field, we use the hourly CODAR data of 66 months during the period from December 2014 to May 2020, combined with GOCI chlorophyll concentration data, to analyze a vital indicator of marine ecological features. From the results of this study, we can understand the ship-measured statistics of ocean currents, real drifter trajectories, high-resolution satellite flow fields, and tidal currents, and changes in ocean chlorophyll concentrations in diurnal, monthly, and seasonal perspectives. This research provides novel and important knowledge for the ocean surface in the north of Taiwan.

1.3. Study Area

The study area is in the northern waters of Taiwan including parts of the TS, the ECS, and the Kuroshio area. The bottom topography of the TS is characterized by a flat, wide, and shallow continental shelf, most of which have a depth of less than 60 m. The ECS shelf is in northern Taiwan with a width of 300 km and an average water depth of 130 m. There is a shelf in I-Lan Bay, and to the east is the

continental slope of the ECS. The water depth exceeds 1000 m. Along the northern coast of Taiwan, there are some tidal stations and current buoys set up by the Central Meteorological Bureau (CWB) of Taiwan, and the Taiwan ocean radar observing system (TOROS) built by Taiwan Ocean Research Institute (TORI). We integrated these data with GOCI and Himawari-8 satellite images to study the variations in ocean chlorophyll and ocean currents in the north of Taiwan. The scope of the research area and the positions of data collection used in this study are shown in Figure 1.

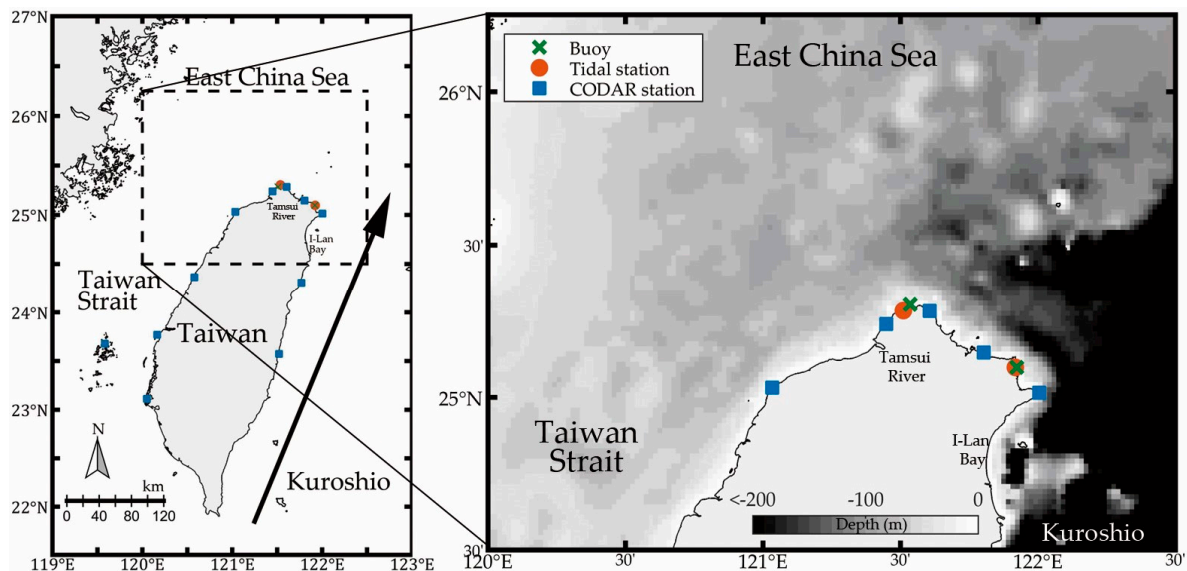


Figure 1. Study area (dotted frame) and adjacent region. The red dot is the tidal station, the green cross is buoy, the blue square is the coastal ocean dynamics applications radar (CODAR) station, and the black arrow is the Kuroshio main path. The background color of the enlarged study area is the submarine topography obtained from the ETOPO1 1 arc-minute global relief model (doi:10.7289/V5C8276M).

2. Materials and Methods

This study used in situ measured ocean current products (historical Sb-ADCP), a Taiwan ocean radar observing system, and two geostationary satellite datasets, including GOCI and Himawari-8. First, we used multi-year statistical and seasonal Sb-ADCP data from 1991 to 2019 and divided them into 15 locations in the northern waters of Taiwan for analysis of the long-term and seasonal ocean surface and underwater current situations. The monthly, seasonal, or long-term ocean current velocity is the arithmetic average of all available data in the month, season, or data span at that grid. Then we collected hourly drifter experimental trajectory data to analyze the type of flow directions and tidal currents which may exist in the north of Taiwan. To understand the relationship between the variations in chlorophyll concentration and the flow field, the monthly average values during the time overlap between CODAR and GOCI data (December 2014 to May 2020) were calculated to obtain the average direction of the flow field and the value of chlorophyll concentration. The CODAR data were distinguished from ebb and flood periods according to the time of the tide period provided by the tidal station. The average flow fields during the ebb and flood periods in each month were then calculated. These calculations were used to investigate the tide phenomenon observed in the drifter experiment. To discuss the long-term (April 2011 to May 2020) changes in chlorophyll concentration, the water in the north of Taiwan was divided into three areas and eight section lines for time series analysis. Finally, a combination of Himawari-8 sea surface temperature (SST) data, GOCI data, and CODAR data were employed to explore the diurnal changes in the chlorophyll concentration in the north of Taiwan. The following subsections present detailed data and its processing.

2.1. Sea Surface Temperature and Chlorophyll Concentration

2.1.1. Geostationary Ocean Color Imager

The GOCI acquires data in eight spectral bands (six visible and two near-infrared) with a spatial resolution of about 500 m over the northeast Asian marginal sea (covers a 2500 square kilometer area centered at 36°N, 130°E) and is one of the three payloads onboard the communication, ocean, and meteorological satellite. The level 2 hourly mass concentration chlorophyll concentration in sea water by ocean color index algorithm data products from April 2011 to May 2020 have been used in this study. The data were obtained from the National Aeronautics and Space Administration (NASA) ocean color web [18]. The observation time in northern Taiwan was 0:00 to 7:00 (UTC) and the local time was 8:00 to 15:00 (UTC+8).

2.1.2. Himawari-8

Himawari-8 is the 8th Himawari geostationary Japanese weather satellite and is operated by the Japan Meteorological Agency. Himawari-8 carries the Advanced Himawari Imager, which features a wide spectral range and 10-min temporal resolution. The research products of SST used in this study were supplied by the P-Tree System from the Japan Aerospace Exploration Agency. The SST data (2 km spatial resolution) were available from 7 July 2015, with a 1-h temporal resolution. The Himawari-8 SST data have successfully been used for diurnal variations [16] and sub-mesoscale vortex tracking [19] in the adjacent waters of Taiwan.

2.2. Ocean Currents

2.2.1. Buoy

The CWB of Taiwan set up a disc-shaped buoy along the coast of Taiwan, which is placed in a fixed sea area with an anchor system. The ADCP from Teledyne RD Instruments is installed at the bottom of the buoy to measure the ocean current downward and observe once an hour. Two buoys, including the Fugui Cape buoy (FGC; 25.304°N, 121.535°E) is located on the north coast of Taiwan where the water depth is 34 m, and the Longdong buoy (LD; 25.098°N, 121.923°E) is located on the northeast coast of Taiwan, where the water depth is 27 m (see Figure 1). Herein, hourly buoy data of the FGC from August 2017 to Dec 2019 and LD from August 2016 to Dec 2019 are used.

2.2.2. Ship-Board ADCP

Historical Sb-ADCP data from 1991 to 2019 were acquired from the Ocean Data Bank of the Ministry of Science and Technology of Taiwan by R/V Ocean Researchers I, II, and III. The instrument used was the ocean surveyor vessel-mounted ADCP manufactured by Teledyne RD Instruments. The frequencies include 75 kHz and 150 kHz. The ocean current data is processed in accordance with the quality control standards of center global temperature-salinity profile program from the National Oceanographic Data Center. The Sb-ADCP data processing method is first to calculate the vessel velocity and the current velocity of each water layer from the original data. Since the velocity measured by Sb-ADCP is the velocity of the ocean current relative to the vessel, the absolute ocean current velocity can be obtained after deducting the vessel velocity. During navigation observation, Sb-ADCP uses bottom tracking mode to measure vessel velocity with the seabed as a reference. Thus, the current velocity measured by Sb-ADCP can be subtracted from the vessel velocity to obtain the absolute current velocity. The available data are then distinguished by the depth of one layer per 10 m, and the data have been transformed to a 0.25° × 0.25° grid for latitude and longitude, respectively.

2.2.3. CODAR

The TOROS along the coast of Taiwan was built by the TORI, National Applied Research Laboratories. The observation instrument is the SeaSonde high-frequency radar system provided by

CODAR Ocean Sensors, and which is a compact, non-contact surface current and wave measurement system. The TOROS is aimed at observing the surface of the ocean. Based on the difference between the observed wave phase velocity and the theoretical phase velocity of deep-water waves, the velocity, and direction of the surface ocean current are calculated. The CODAR can measure ocean surface currents around Taiwan over 100 km from the coast with a 10 km spatial resolution and 1-h temporal resolution. There are 11 CODAR stations around Taiwan and five of them located in northern Taiwan were used in this study (Figure 1), including the Caoli station (LILY; 25.283°N, 121.606°E), the Liukuaicuo station (LIUK; 25.240°N, 121.448°E), the Chaojing station (CIAO; 25.147°N, 121.803°E), the Datan station (DATN; 25.032°N, 121.033°E), the San Diego station (SDGO; 25.015°N, 122.005°E), the Siaqueike station (TUTL; 24.362°N, 120.577°E), the Hoping station (HOPN; 24.306°N, 121.771°E), the Mailiao station (MYLA; 23.768°N, 120.165°E), the Houliiao station (OHAL; 23.677°N, 119.582°E), the Luye station (LUYE; 23.573°N, 121.522°E), and the Peiti station (PETI; 23.112°N, 120.052°E). A high-resolution hourly surface current map is produced from two sets of operational 5 MHz and nine sets of 13/24 MHz compact type high-frequency ocean radar instruments. The CODAR data were used to discuss the ocean phenomena of the current fields north of Taiwan, and the data were also compared with the GOCI and Himawari-8 data. The data time span used in this study was from December 2014 to May 2020. The monthly ocean current velocity is the arithmetic average of all available data in the month at that grid.

2.3. Tide

The CWB of Taiwan set up tidal stations along the coast of Taiwan, with a high-quality liquid-level determination system (Aquatrak 4100), which is provided by the Aquatrak Corporation. Tides are measured in centimeters from the instrument reference level of a tide station. The instrument reference level of each tide station is calibrated to a tide gauge benchmark beside the station. The mean sea level of Keelung (25.155°N, 121.7522°E) is treated as the zero datum level for the Taiwan area (Taiwan Vertical Datum 2001). Tides from two tidal stations, including the Linshanbi tidal station (LSB, located at 25.28389°N, 121.5103°E) locates on the north coast of Taiwan, and the Longdong tidal station (LDT, located at 25.0975°N, 121.918056°E) locates on the northeast coast of Taiwan, were used in this study (see Figure 1). Herein, the hourly tide gauge data of LSB from December 2014 to May 2020 and hourly tide gauge data of LD from August 2016 to May 2020 are used.

2.4. Drifter

The drifter observation data were obtained from the Global Drifter Program (GDP) of the National Oceanic and Atmospheric Administration Atlantic Oceanographic and Meteorological Laboratory Physical Oceanography Division. Drifters sit at the surface of the ocean and are drifted via near-surface ocean currents. Ocean surface current velocities are calculated by the change in position of the drifter over time. GDP buoy data are available in three formats, including real-time data, six-hourly interpolated data, and hourly interpolated data. The drifter velocities of hourly interpolated data are derived from the temporally nonuniform data set of locations [20]. This data set is a tool for the study of relatively small-scale, tidal wave, and high-frequency oceanic processes. Ten drifters which passed through the study area were used in this study, including ID numbers 61501380, 61502320, 62325980, 62415670, 62416680, 63894830, 63942860, 63942870, 63942890, and 63943580.

3. Results

3.1. Characteristics of Ocean Current in Northern Taiwan

3.1.1. Historical Survey Observation

From the ocean current observation results in the surrounding waters of northern Taiwan, there are northward near-surface flows for both the TS and the Kuroshio regions under multi-year statistics

(Figure 2), with 0.56 m/s and 0.99 m/s, respectively. There were two branches in the northwest of Taiwan: one flow continued northward (0.4 m/s) to the ECS, while the other gradually deflected eastward (0.25 m/s) along the northern coast of Taiwan in the ECS shelf. Judging from the seasonal statistics, such situations mostly occurred in spring (March to May) and summer (June to August). There was a flow from east to west on the northeast of Taiwan (opposite to the flow in spring and summer) in fall (September to November), and this flow is faster and wider in winter (December to February). We divided the coastal area of northern Taiwan, which is where the flow field is the most irregular, into 15 areas to analyze the vertical current profile from the near surface to a depth of 70 m (Figure 3a). The changes in the entire layer currents show that the direction of the near-surface current could be inconsistent with lower depths, however, this study is focused on the changes in the near-surface current, and the following discussion is based on the flow field at a 10-m depth (Figure 3b–d).

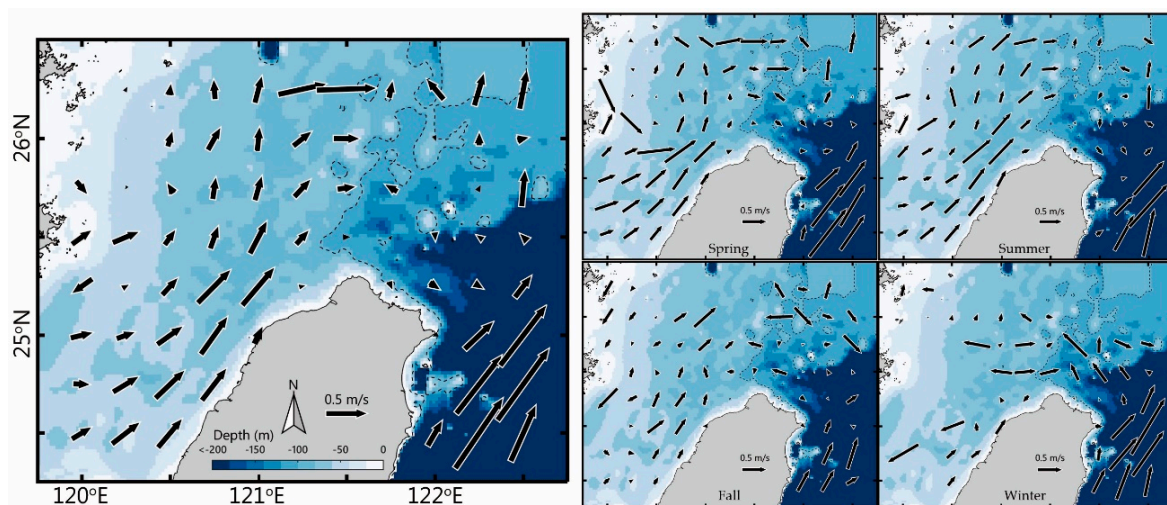


Figure 2. Historical in-situ survey observational ocean 10-m flow field, including multi-year statistics and the four seasons. Black arrows show the ocean current, the blue background is the seabed topography, and the black dotted line is the 100-m isobath.

First, regarding the flow situations near the TS (A1, B1, and C1), the direction of flow in the near-shore region (C1) ranges from NNW to NE in each season, but the flow velocity varies greatly, reaching 0.80 m/s in summer and only 0.14 m/s in winter. The flow in the B1 area was northeastward in spring (0.35 m/s) and summer (0.63 m/s) and northwestward in fall (0.26 m/s) and winter (0.46 m/s). The northeastward flow occurred in the A1 area in all seasons, and the slowest flow velocity was in winter (0.12 m/s). Next, regarding the flow situations in areas A2, B2, and C2, there was an obviously different direction of flow in the coastal area (C2). The flow direction in spring and summer was ENE (0.18 m/s), and the direction in fall and winter was between SSW and SW (0.11 m/s). In the B2 area, the westward flow occurred in fall but in other seasons this was in a northeast direction. The northeastward flow occurred during the whole year in the A2 area. In general, the flow field which is close to the TS side is in a northeastward direction in spring and summer, while southwestward flow occurred in the fall and winter near the coastal area. Regarding the north of Taiwan (A3, B3, and C3), the northeastward flow (0.1 m/s) occurred near the coast (C3) in all seasons. In the A3 and B3 regions, there was a different flow direction in each season. It could be speculated that there exist complicated currents, and that would be discussed with coastal radar currents data in Section 3.2.1. About the western waters of Taiwan (A4, B4, and C4), the southeastward flow (0.1 m/s) existed near the coast (C4) for the whole year. In the B4 area, both the southeastward flow occurred in spring and summer, but the northwestward flow occurred in fall and winter. There was a southward flow in the area of A4 in summer and fall, but this was northwestward in spring and winter. Focusing on the areas which are close to the Kuroshio region (A5, B5, and C5), the southeastward flow occurred near the coast (B5 and C5) in spring, summer and fall, but flowed northwestward in winter, which could be related to the

Kuroshio invasion to the ECS shelf in winter [13]. The different flow directions occurred in each season in the A5 area.

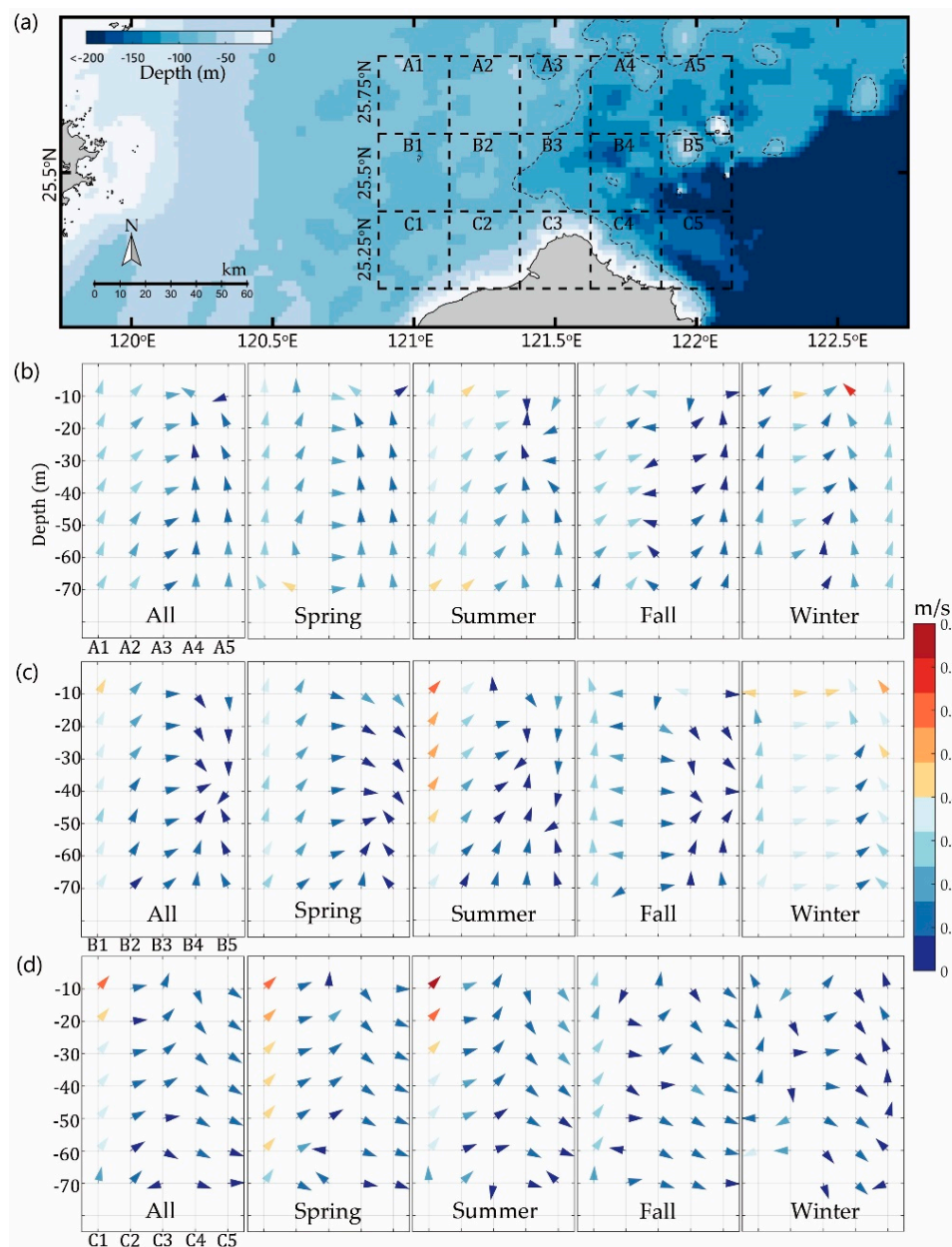


Figure 3. Multi-year statistics and seasonal results of the vertical profile (10–70m depth) of ocean currents in northern Taiwan: (a) Fifteen specific analysis locations, (b) areas A1 to A5, (c) areas B1 to B5, and (d) areas C1 to C5.

It can be found from the historical Sb-ADCP results that there is an obvious eastward coastal flow in northern Taiwan in spring and summer, but there are irregular flow directions in fall and winter, which are eastward or westward along the coast. Detailed results for the aforementioned flows can be found in Table A1 of Appendix A. The flow situation in the north of Taiwan can be understood via the historical flow field data. However, we should note that these results were based on Sb-ADCP during survey observations and that this dataset does not feature a continuous measurement in each area. Therefore, these results could not be decisively judged in terms of whether these were correct in each region. In Section 3.2.1, a comparison is made with the CODAR current results to find more complete long-term flow situations in the north of Taiwan.

3.1.2. Drifter Experiments

In the previous section, historical Sb-ADCP data provided possible flow field conditions in the north of Taiwan. In this section, 10 drifter trajectories are discussed. Ten drifter experiments were divided into four cases to discuss the trajectories and velocities. What is important, however, is that through these experiments we may understand that the influence of the tidal current is an important and critical factor in the complicated flow field of northern Taiwan. The four classifications of the drifter experiments were as follows: The drifter placed in the TS in summer (Figure 4), winter (Figure 5), and spring (Figure 6), and the drifter placed in the Kuroshio region in winter and spring (Figure 7).

It can be seen that two drifters were released from the TS and the other drifter was released off the coast of northwestern Taiwan in August 2014 (Figure 4a). Three drifter trajectories moved along the coast to the northeast corner of Taiwan, which is consistent with the seasonal long-term results observed by Sb-ADCP (Figure 2). It is worth noting that the drifter presented a strong tidal movement trajectory type in northern Taiwan. The drifters continuously moved eastward and westward during the tide period; therefore, they continued moving for a long time near the northern coast. The first drifter (ID: 61501380) in the northern area, with 0.31 m/s for 200 h (Figure 4b). Affected by the tidal current, the eastward speed of the drifter was 0.39 m/s (96 h) and the westward speed was 0.23 m/s (104 h). The trajectory of the second drifter (ID: 61502320-1) was along the northern coast, revolving around the north at 0.55 m/s for 249 h (Figure 4c), the eastward speed of the drifter was 0.57 m/s (142 h) and the westward speed was 0.53 m/s (107 h). The third float (ID: 61502320-2) was released near the coast and was obviously affected by the tidal current in the beginning. It moved quickly along the west coast (1.34 m/s), moving eastward for 15 h (1.38 m/s) and then drifting westward for 15 h (1.30 m/s). On the east coast (0.34 m/s), the eastward speed of the drifter was 0.40 m/s (47 h) and the westward speed was 0.27 m/s (42 h), then it drifted near the cape (0.14 m/s) in the end. These experiments provide important results, i.e., that the flow in northern Taiwan indeed moves along the northern coast in summer and it has a significant movement characteristic in accordance with the tidal period.

The second experiment released three drifters in the TS in February 2017 (Figure 5). These were respectively released between 25.5°N to 26°N in the TS, but the drifting processes all took more than one month and revolved back to the northeastern coast of Taiwan. All drifters were significantly affected by the tidal currents. After the first drifter (ID: 62325980) was released, it first drifted southward to northwestern Taiwan and then drifted northward and revolved for 418 h in northern Taiwan (Figure 5b). Affected by the tidal current, the eastward speed of the drifter was 0.66 m/s (217 h) and the westward speed was 0.60 m/s (201 h). The release time of the second drifter (ID: 62415670) in the Taiwan Strait was only one hour later than that of the first drifter, and the released position was slightly to the north. The drifter also drifted southward and then drifted northward to northern Taiwan, then it revolved in northern Taiwan for 639 h (Figure 5c). Affected by the tidal current, the eastward speed of the drifter was 0.57 m/s (325 h) and the westward speed was 0.54 m/s (314 h). The third drifter (ID: 62416680) was released slightly north and 12 days later than the first drifter. However, the drifting time from the start to the northeast coast of Taiwan was only 1 day later than the first drifter, the eastward speed of the drifter was 0.68 m/s (98 h) and the westward speed was 0.56 m/s (80 h) in northern Taiwan. This experiment provided some important results, i.e., that the nutrients or other substances in the TS could move from the Kuroshio region to northeastern Taiwan in winter via water exchange via the geostrophic and the tidal currents.

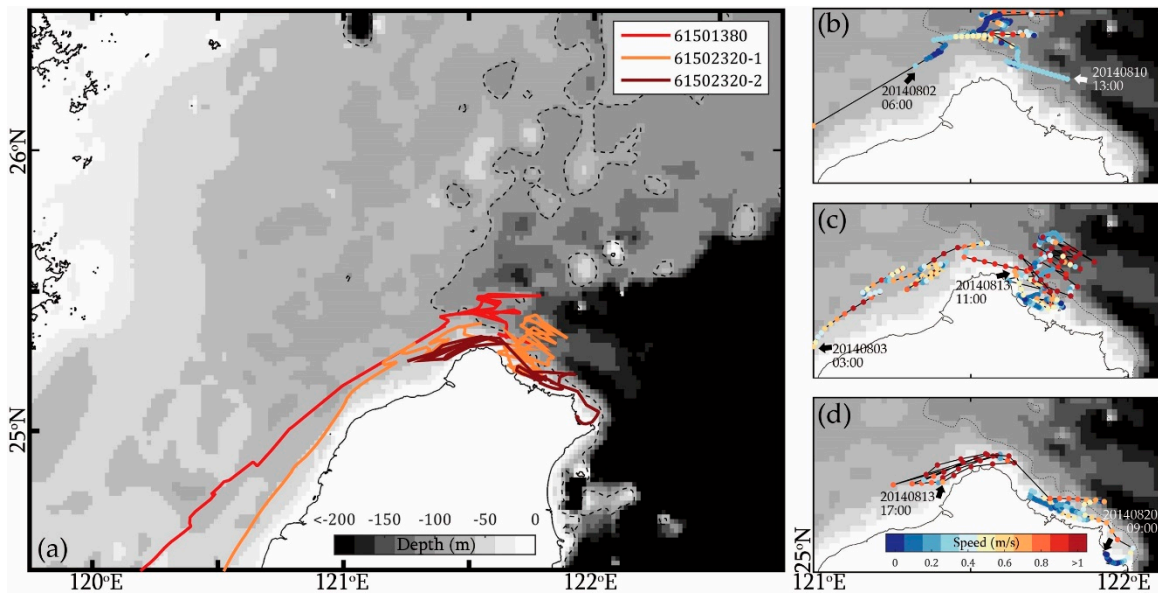


Figure 4. (a) Three trajectories of drifters in the Taiwan Strait in summer. (b) ID: 61501380, (c) ID: 61502320-1, and (d) ID: 61502320-2.

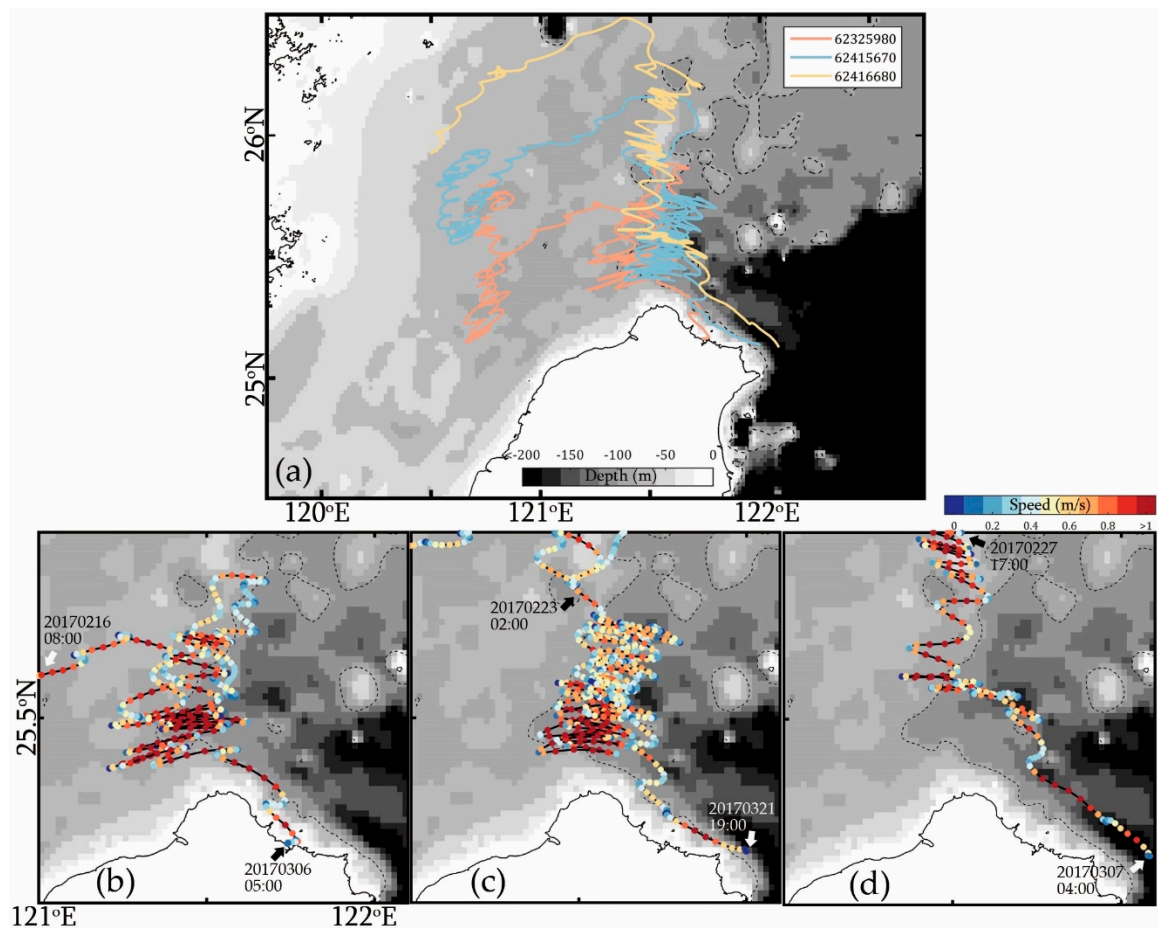


Figure 5. (a) Three trajectories of drifters in the Taiwan Strait in winter. (b) ID: 62325980, (c) ID: 62415670, and (d) ID: 62416680.

The third experiment released two drifters in the TS in March 2017 and one drifter near the northern coast in April 2017 (Figure 6). The first drifter (ID: 63942860) entered northern Taiwan and was

also affected by the tidal current. It drifted around a large circle to the northeast corner of Taiwan and then continued northward along the Kuroshio path (Figure 6b). The speed of the drifter was 0.57 m/s when it drifted northward on the west side of northern Taiwan, and it was 0.41 m/s when it drifted southward on the east side, and the velocity could reach 1.22 m/s along the Kuroshio path. The second drifter (ID: 63942870) was released along the northern coast, which drifted southward along the coast into the I-Lan Bay and then moved to the Kuroshio path (Figure 6c). The drifting trajectory was like the first drifter, with an average speed of 0.39 m/s along the coast, where the fastest velocity was 0.96 m/s after entering the Kuroshio path. The release position of the third drifter (ID: 63942890) was close to the first drifter. However, the subsequent trajectories of the two drifters were quite different. This drifter did not move southward to the northern coast of Taiwan but instead drifted slowly eastward at a speed of 0.29 m/s. The results of this experiment showed that drifters which enter northern Taiwan at a similar time may have hugely different trajectories. The southward drifter east of Taiwan could be brought to the north by the strong Kuroshio Current off the northeast coast of Taiwan.

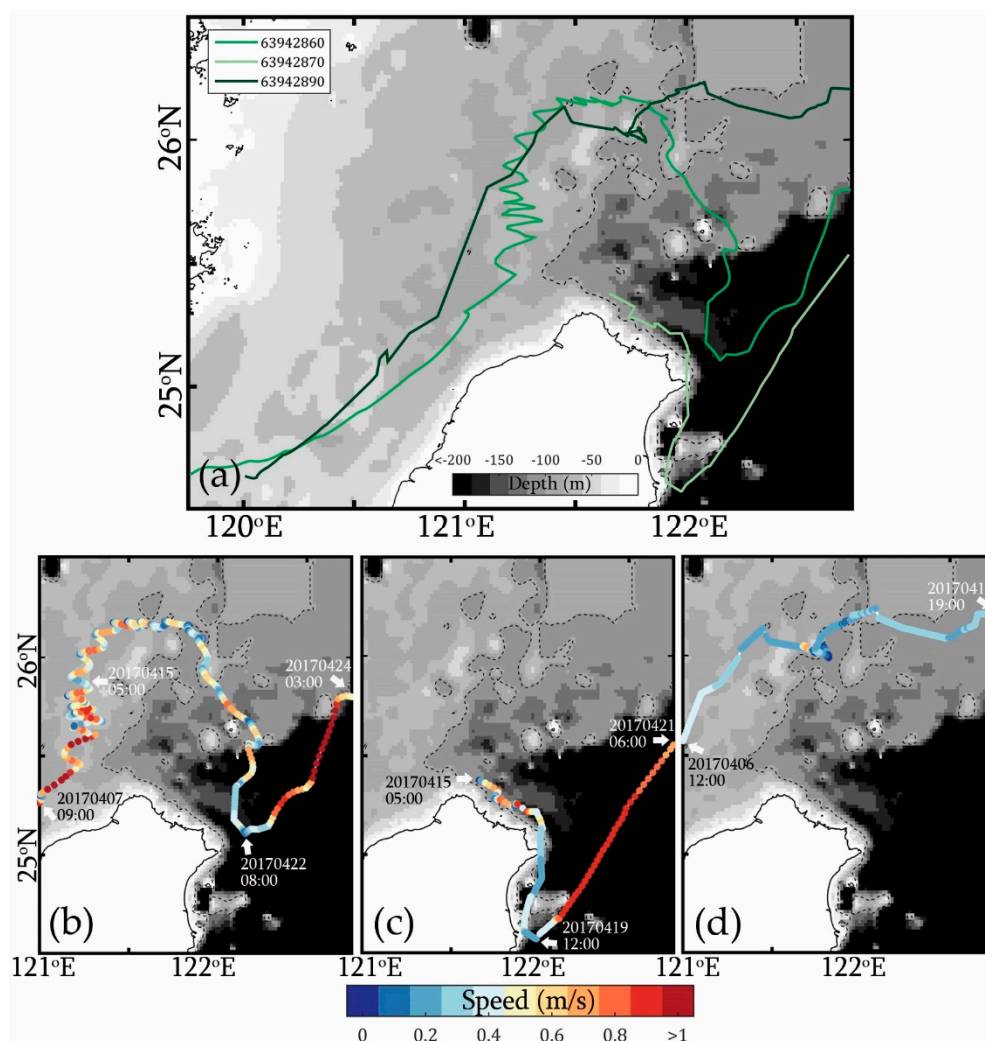


Figure 6. (a) Three trajectories of drifters in the Taiwan Strait in spring. (b) ID: 63942860, (c) ID: 63942870, and (d) ID: 63942890.

The final experiment released two drifters in the Kuroshio region near eastern Taiwan (Figure 7). The first drifter (ID: 63894830) moved northward, following the Kuroshio Current in December 2016, and then drifted westward into northern Taiwan and continued to drift northward (Figure 7b). The second drifter (ID: 63943580) also followed the Kuroshio Current in March 2017 then drifted

westward and finally moved southward to the coast due to the significant tidal current. This result showed that the Kuroshio Current could invade the ECS shelf in winter and spring.

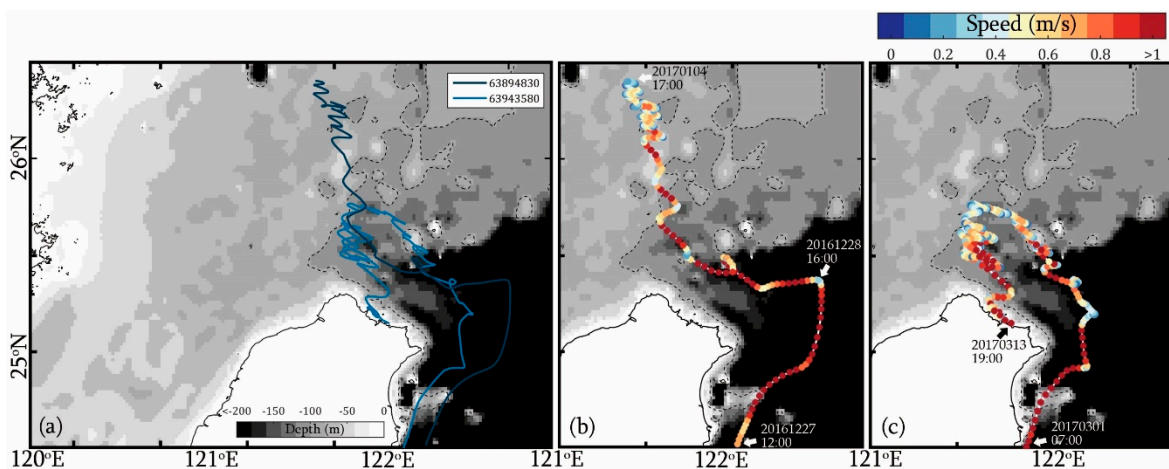


Figure 7. (a) Two trajectories of drifters in the Kuroshio region in winter and spring. (b) ID: 63894830 and (c) ID: 63943580.

In this section, we used historical Sb-ADCP data and drifter experiment analysis to reveal that there are complex flow field variations in the north of Taiwan, especially strong tidal currents. To understand the source for the variations in the ocean chlorophyll concentration, it is necessary to conduct continuous and high temporal resolution flow field observations in the study area. Therefore, we present the results of the flow field by coastal radar observation used to analyze the change in chlorophyll concentration from diurnal to seasonal perspectives in the next section.

3.2. Diurnal to Seasonal Changes in Chlorophyll Concentrations

3.2.1. Monthly to Seasonal Variations

To understand the variations in the flow field in northern Taiwan, this section demonstrates the observations of the CODAR ocean current data from December 2014 to May 2020. The monthly flow field and the monthly average chlorophyll concentration are presented in Figure 8. The flow field is particularly chaotic during the seasonal transition in March and October in northern Taiwan. Based on the results of the CODAR flow field for each month, the definition of the summer season was June to September and the fall season was October and November. In the TS, east of Taiwan, the flow field flowed northward in spring and summer, and flowed southward in fall and winter. On the west side of Taiwan is the Kuroshio Current, which flowed northward all year round. Appendix A Table A2 lists the analysis results of the flow field with 15 grid points (see Figure 3). The results show that the flow of northern Taiwan mainly flowed eastward along the coast in spring and summer with velocities of 0.11 m/s and 0.15 m/s, respectively, therefore, the water in the TS flowed to the Kuroshio region. The water flowed westward along the coast in winter (0.08 m/s) and the water in the Kuroshio region flowed to the ECS and TS. In fall, the flow field was irregular, where the coastal water on the west side flowed westward and the coastal water flowed eastward on the east side.

It can be seen here that the flow direction and velocity statistics in each season from the CODAR observations are more consistent than those of the Sb-ADCP data. The CODAR system observed the ocean flow every hour and it could completely analyze the tidal current characteristics in northern Taiwan, but we can only obtain the situation at a specific moment from the Sb-ADCP data. Figures 9 and 10 present the flow field distributions during the ebb and the flood periods, respectively. The tidal period was determined based on the change of the water gauge at the LSB tidal station. Regardless of the season, the current flowed eastward during the ebb period and flowed westward during the flood period in northern Taiwan. The flow velocity in the ebb period was 0.43 m/s in summer and 0.27 m/s

in winter. The seasonal characteristic of flow velocity was opposite in the flood period, which was 0.26 m/s in summer and 0.45 m/s in winter. For detailed data analysis, please refer to Appendix A Tables A3 and A4. With continuous observations of the flow field data, it could be understood why the drifter experiment in the previous section produced various results, and why the drifter in northern Taiwan drifted eastward and westward, then revolving for a long time.

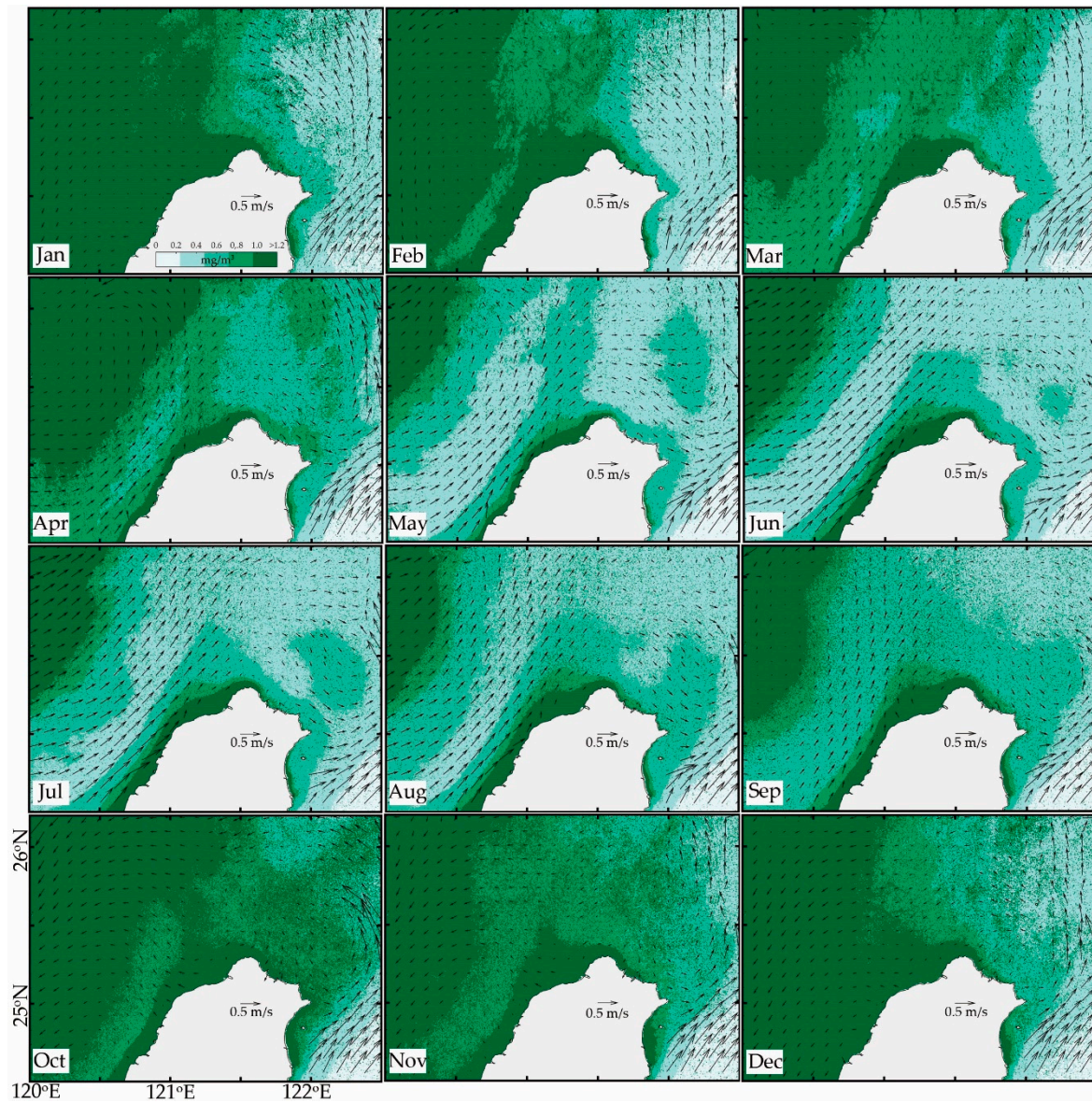


Figure 8. Monthly chlorophyll concentration from December 2014 to May 2020 with the CODAR flow field.

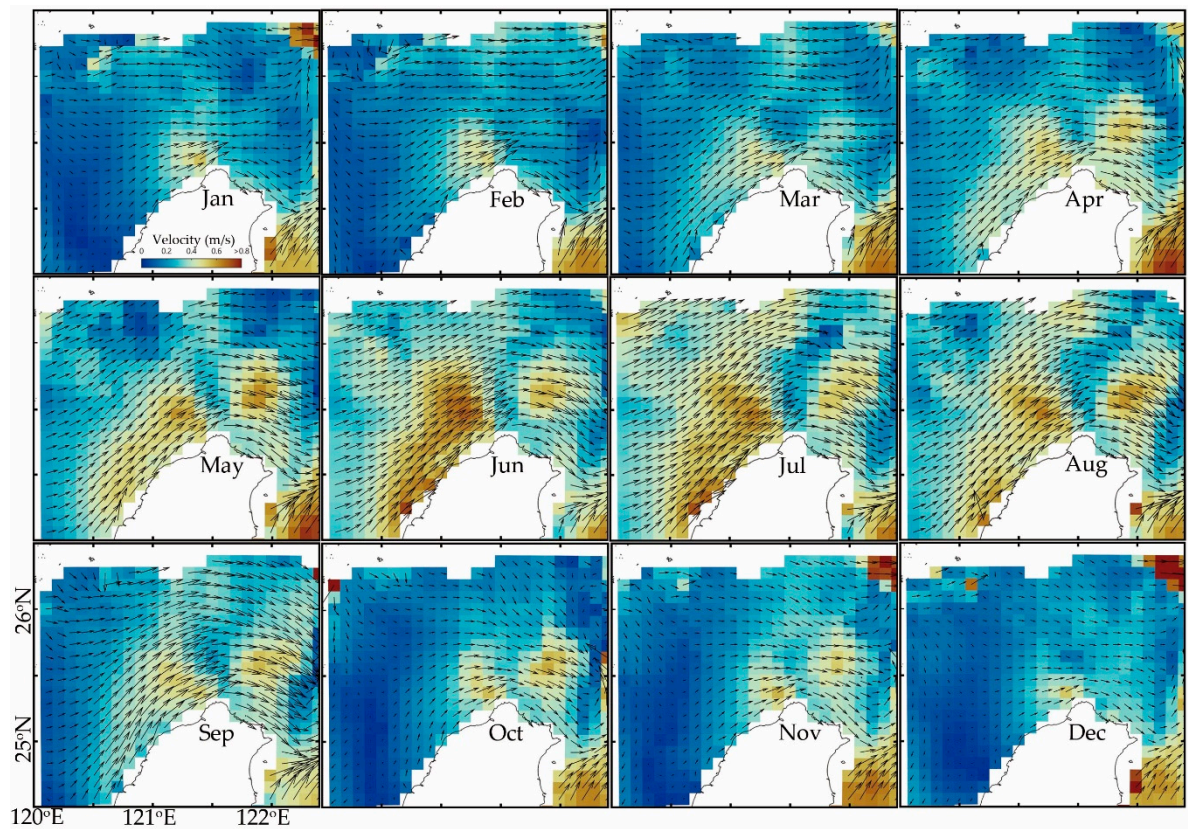


Figure 9. Monthly CODAR flow field during the ebb period from December 2014 to May 2020.

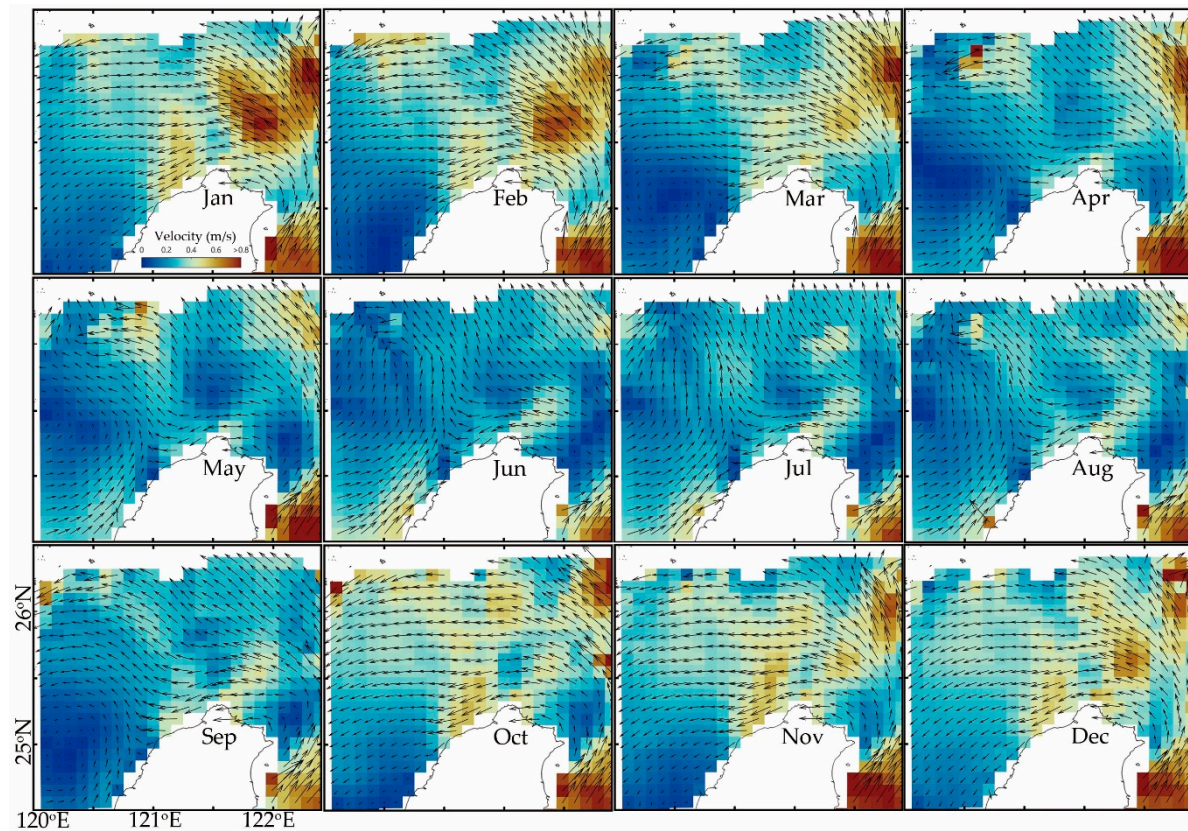


Figure 10. Monthly CODAR flow field during the flood period from December 2014 to May 2020.

Here, we focus on the monthly to seasonal chlorophyll concentration changes in the northern waters of Taiwan (Figure 8). The chlorophyll concentration in the north of Taiwan could be affected by the effects of different water systems in different seasons, making the marine environment dynamic, and the distribution of nutrients and fishing resources would also have seasonal variations. Even if there is an island mass effect via the Kuroshio Current and island interaction that enhances some nutrients in the Kuroshio region [19], the overall chlorophyll concentration is still low relative to the TS. In fall and winter, the coastal waters of the Yangtze River carry high amounts of nutrients along the coast of China. The northeast monsoon and the China Coastal Current expand the water southward to the TS, which is one of the important reasons for the high ocean productivity on the west side of northern Taiwan [21]. According to the observation results from the CODAR data, the Kuroshio flow path gradually invaded the ECS shelf from October. In winter, the Kuroshio region has high SST and low nutrients, and the TS has low SST and high nutrients. The low nutrient Kuroshio water gradually flowed into the TS, forming a chlorophyll front in northern Taiwan. The chlorophyll concentration in February (Figure 8) clearly presented the front and low nutrient water intrusion into the flow channel of the TS. From the beginning of spring, the Kuroshio branch current, from the north of Luzon Strait, began to increase its velocity in the TS, and the Kuroshio branch invaded from the east of Taiwan to the ECS, began to disappear. In March, a clear seasonal transition period in the flow field can be seen. From April to the end of summer, the flow direction of the northern Taiwan waters changed to the east, and the high nutrient substances poured into the ocean in western Taiwan began to flow into the Kuroshio region along the coast. From June to September, a cold dome may form in the offshore waters of northeastern Taiwan [13]. The cold dome would raise the bottom nutrient substances to the ocean surface, increasing the chlorophyll concentration. It can be seen that there is a circular high concentration area off the northeastern coast of Taiwan in July.

Next, we further explored the changes in the chlorophyll concentration from the northern coastal area to the waters of I-Lan Bay. Figure 11 presents long-term chlorophyll concentration from April 2011 to May 2020 and shows three analysis areas and eight observation sections. The visualized L1 to L8 sections present obvious seasonal and spatial changes (Figure 12a,b). Area A is located at the junction of the northern end of the Taiwan Strait and the northern waters of Taiwan, and the seasonal changes in the chlorophyll concentration are obvious (Figure 12c). The average chlorophyll concentration from November to January exceeds 2 mg/m^3 , and the lowest average concentration in spring is only 1.4 mg/m^3 . In summer, the concentration along the coast is also high, most likely due to the river pouring into the sea during the flood period. The chlorophyll concentrations in areas B and C are high from August to December, but the causes are different there. The high concentration in August and September is mainly because the ocean currents carry the nutrients produced from the western coast and cold dome [13]. In October to December, this could be due to the backflow of the Kuroshio Current during the time it invaded the ECS shelf in northeastern Taiwan (Figure 8). Judging from the yearly statistical trend, the chlorophyll concentration in northern Taiwan changed little, the concentration in area A was between 1.6 and 2.0 mg/m^3 , and that in areas B and C was between 0.7 and 1.0 mg/m^3 . Figure 13 more clearly presents the changes in the chlorophyll concentration along the coast for each month from April 2011 to May 2020. High-concentration areas mostly exist from the 50 m isobath to the coast. The amount of chlorophyll concentration on the ocean surface would also affect fish activity, in addition to representing the basic productivity of the ocean. The spatial distribution of the concentration in fall to winter and summer changes significantly. The high concentration of chlorophyll ($>1 \text{ mg/m}^3$) in fall and winter diffused to the entire northern sea area, while the high concentration on the 100-m isobath in summer is scarce, and a clear contrast can be found from July and October in Figure 13.

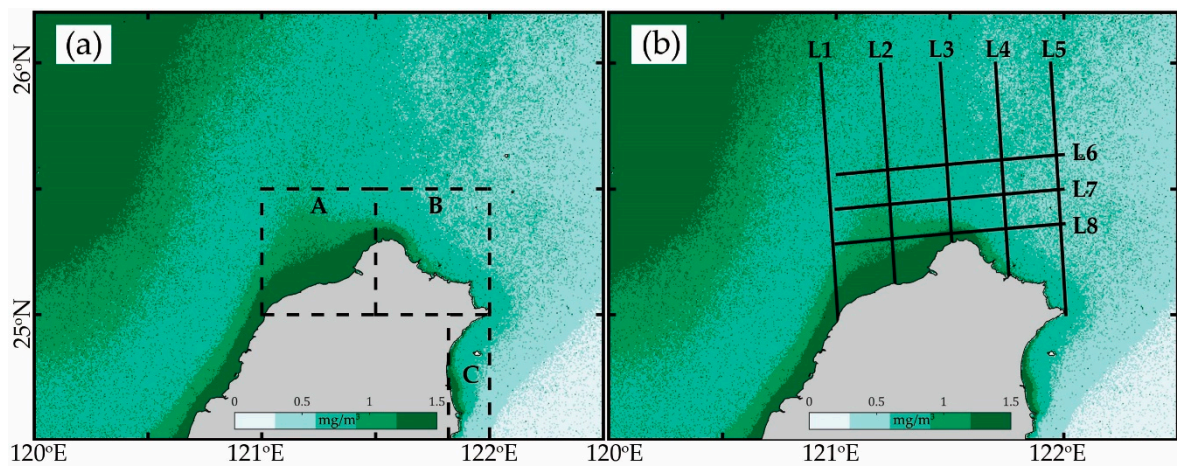


Figure 11. Long-term chlorophyll concentration map from April 2011 to May 2020 and observation area: (a) A (121–121.5°E; 25–25.5°N), B (121.5–122°E; 25–25.5°N), and C (coast; 122°E, 24.5–25°N), (b) L1 to L8 section line.

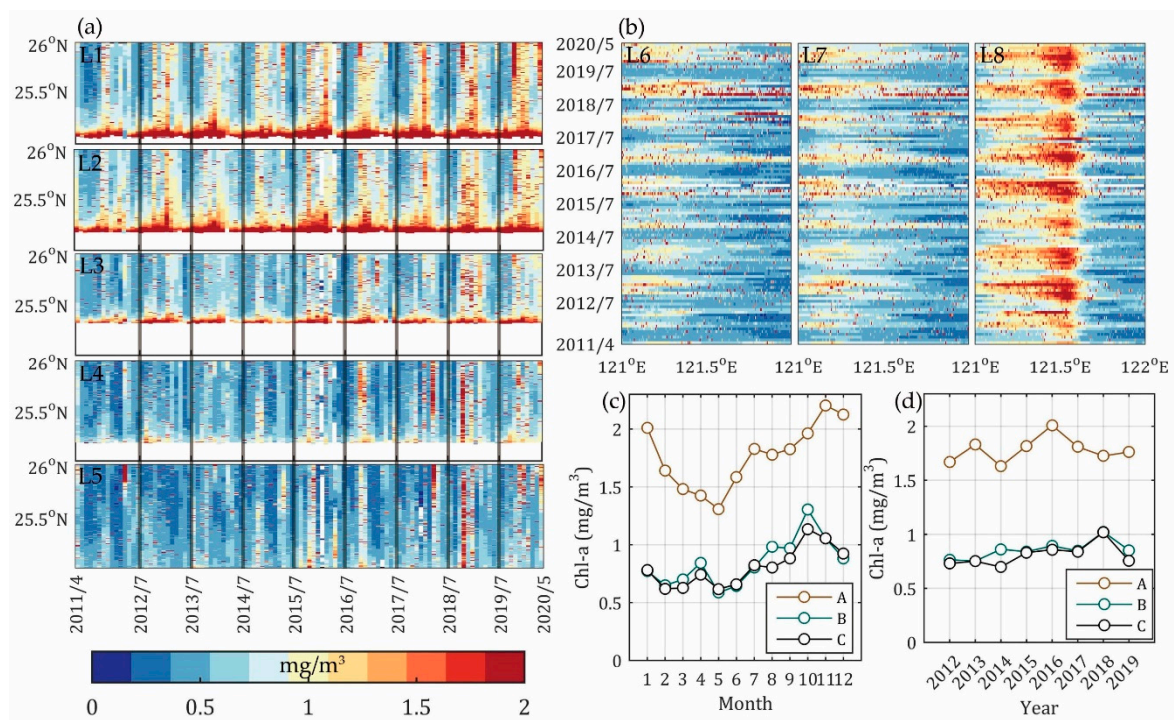


Figure 12. Monthly to seasonal variations in the chlorophyll concentration. (a) L1 to L5 sections, (b) L6 to L8 sections, (c,d) monthly and yearly means of the three areas in Figure 11a.

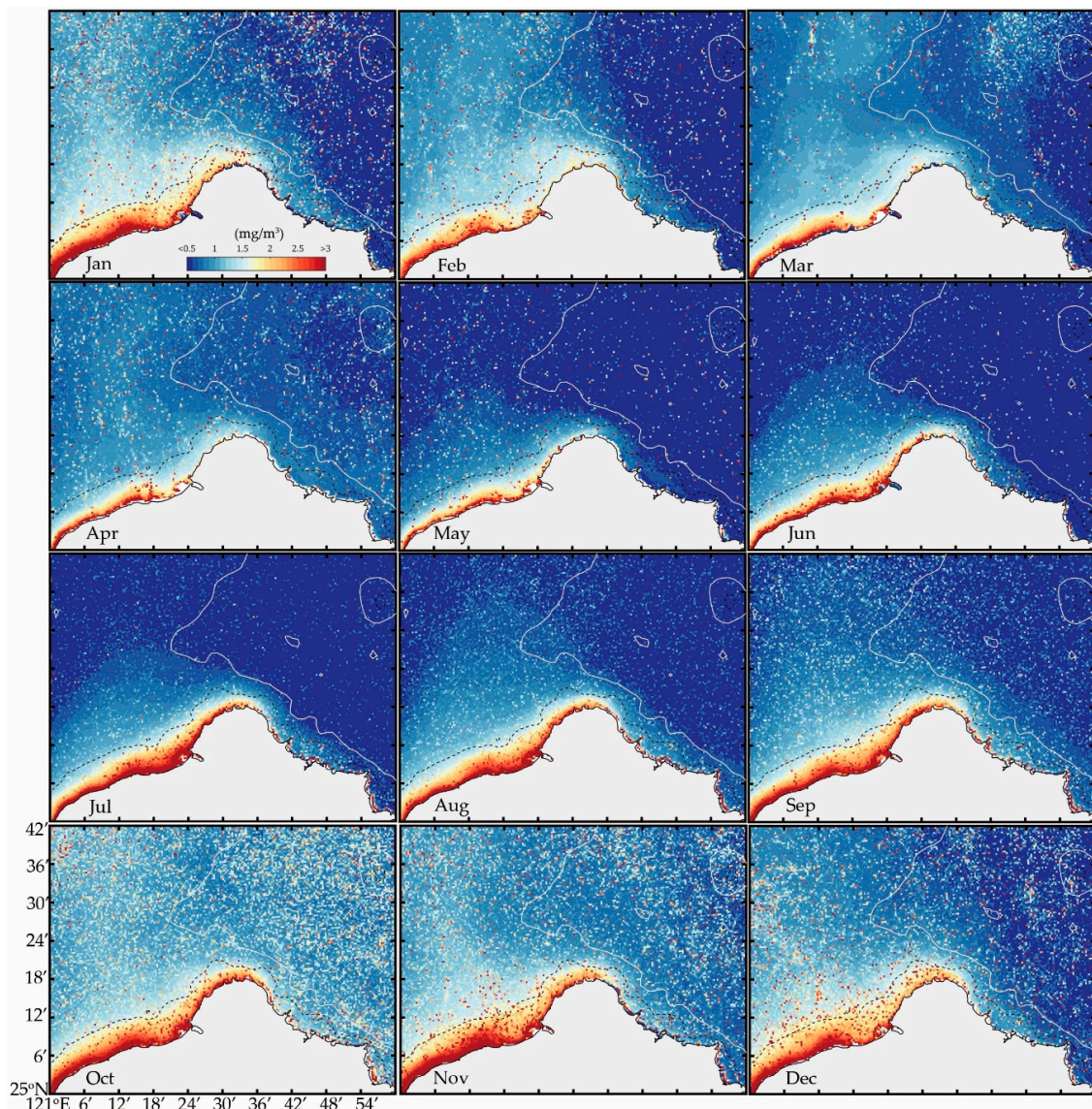


Figure 13. Distribution of the monthly average chlorophyll concentration from April 2011 to May 2020 along the northern coast of Taiwan. The black dotted lines and the white line segments represent the 50 m and 100 m isobaths, respectively.

3.2.2. Diurnal Variation with Tidal Currents

In the previous section, we learned about the seasonal and long-term changes in the chlorophyll concentration along northern Taiwan. Here, in this section, we want to understand the short-term coastal variations. We used two cases in winter and summer to illustrate the effect of tidal current on the chlorophyll concentration and SST. Figure 14 shows the flow field, chlorophyll, and SST from 1:00 to 7:00 (UTC) on 19 February 2016. The three blocks along the coast (A, B, and C) were used to monitor changes in the sea surface characteristics. During these 7 h, the tidal currents first moved westward and then turned eastward. With the westward flow during the flood period, the high SST water flowed in from the east coast of the three areas and this lasted for three hours. The tidal pattern turned to the ebb period and flowed eastward at 4:00, where the water gradually cooled down the chlorophyll concentration increased in the three areas. Detailed data show that the chlorophyll concentration in area A decreased from 2.56 mg/m^3 to 1.96 mg/m^3 and then increased to 3.4 mg/m^3 . The concentrations in areas B and C also decreased first and then increased by nearly 2-fold. The change of SST ranged from $0.6 \text{ }^\circ\text{C}$ to $1.0 \text{ }^\circ\text{C}$ in the three areas.

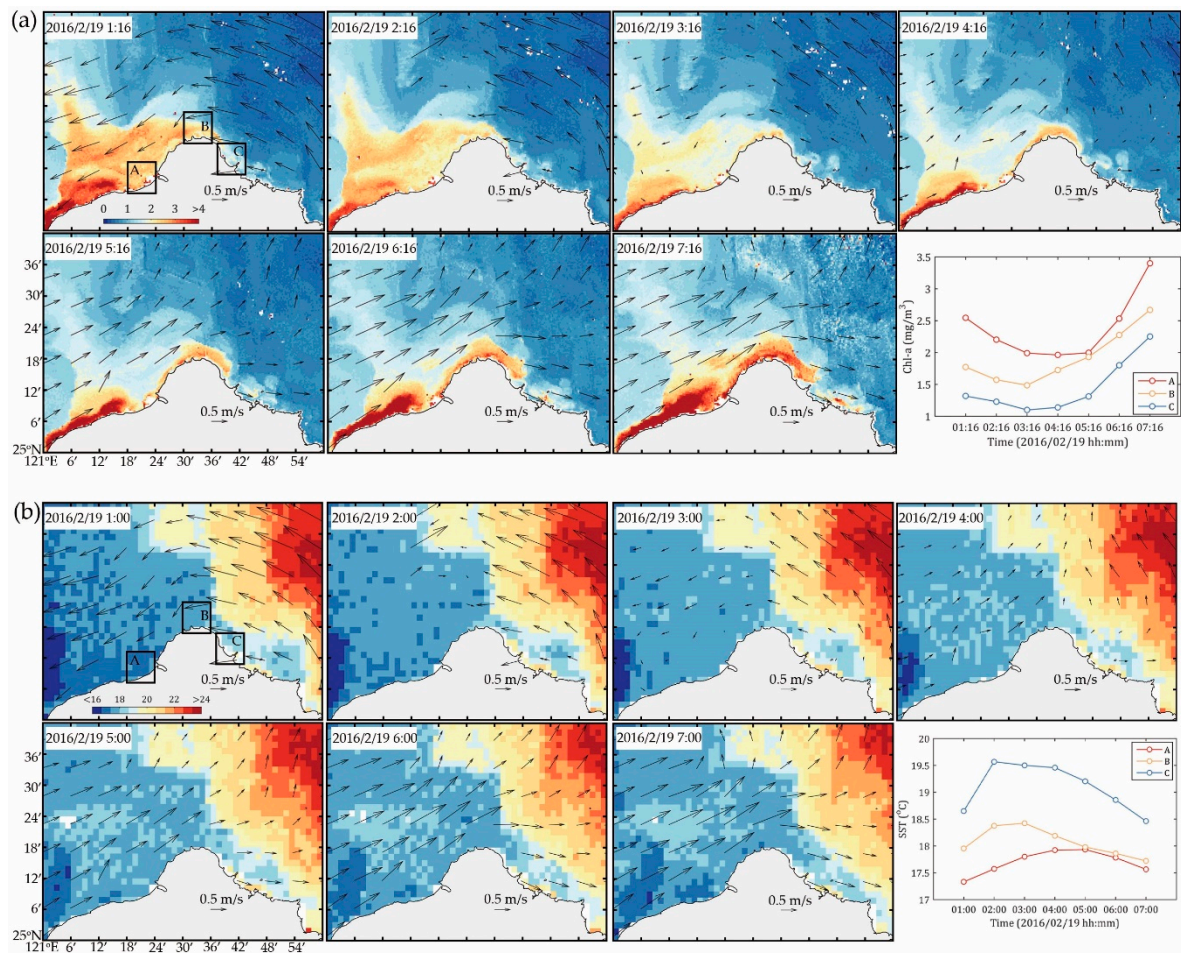


Figure 14. Short time period of (a) chlorophyll concentration and (b) SST variations with ocean currents from Feb 19, 2016, 1:00 to 7:00 (UTC). The areas A, B, and C in the time series diagram were selected as black boxes inside the map.

The second example is from 0:00 to 7:00 (UTC) on 20 July 2017 (Figure 15). The flow pattern in the first five hours was an eastward flow during the flood period, and the latter two hours are converted into the ebb period and flowed westward. It can be clearly seen that there is an area with a high chlorophyll concentration and high SST in the west coast which flowed eastward along the coast in five hours. The chlorophyll concentration in area A decreased from 4.38 mg/m³ to 2.42 mg/m³ in three hours, increased from 0.98 mg/m³ to 1.43 mg/m³ in area B, and did not change much in area C, because the high-concentration substances carried by the tidal currents turned back before arriving. The change in SST in area B is the most obvious, rising from 30.1 °C to 31.1 °C within five hours.

From these two cases, it can be found that the influence of the ebb and flood currents in the northern waters of Taiwan could cause the chlorophyll concentration near the coast to change greatly in a short amount of time. This is also supported via the combined geostationary satellite ocean color from GOCI and the SST from Himawari-8 with the ocean currents from the CODAR system, and these are particularly useful remote sensing tools for the entire Taiwan coastal environmental monitoring society, and innovative marine science issues will be discussed in the future.

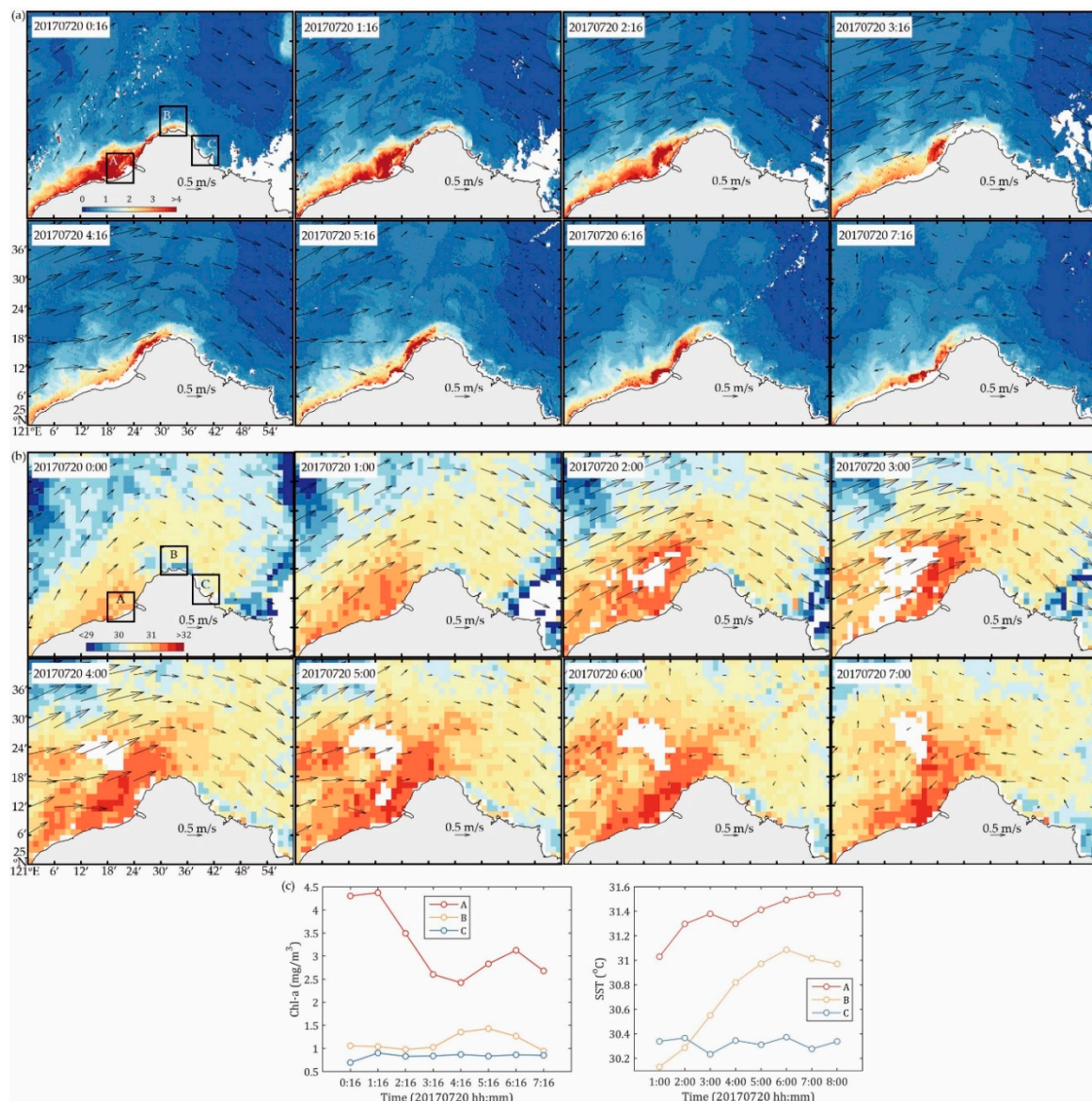


Figure 15. Short time period of (a) chlorophyll concentration and (b) sea surface temperature (SST) variations with ocean currents from July 20, 2017, 0:00 to 7:00 (UTC). The areas A, B, and C in the (c) time series diagram were selected as black boxes inside the map.

4. Discussion

4.1. Current Trajectory Tracking Experiment

We have used CODAR data to gain a new understanding of the water exchange process in the northern waters of Taiwan, including seasonal changes with significant tidal variations. In this section, we use the ocean current data from CODAR to simulate the trajectories of drifters. The drifting trajectory cannot completely correspond to all the movements of ocean chlorophyll via currents, but we can clearly know the possible flow direction distribution. A virtual drifter trajectory could be used to illustrate the flow field characteristics mainly observed in northern Taiwan to facilitate the discussion of future scientific research topics. Figure 16a shows the characteristics of the main summer flow field which flowed eastward from the TS to the Kuroshio region. As the drifter progresses, it could be stagnated by tidal currents in northern Taiwan. Figure 16b shows the two flow branches in northern Taiwan, where one branch flows along the coast to the east of Taiwan and the other branch continues northward, however, the mechanism between these two branches is still unclear. Figure 16c illustrates

that the trajectory of a drifter released at the same position but at a different time would change greatly due to subsequent variations in the tidal currents. Even if the final drifter would go to the Kuroshio region, the elapsed time difference could be huge. Figure 16d shows that the water in the Kuroshio region in winter could mix with the ECS water as the Kuroshio Current invades the shelf. Figure 16e,f show the main patterns of the winter flow field in northern Taiwan. The water on the west coast of Taiwan flowed southward, and the water on the east coast of Taiwan moved into the ECS.

To summarize, the flow field in northern Taiwan is quite complicated, and the effect of the tidal current is significant. The water in the TS could indeed mix the ECS water with the Kuroshio waters, which confirms the previous study [13]. Driven by the tidal currents all year round, there are water exchange processes with different characteristics in northern Taiwan. The above six virtual drifters present the characteristics of the flow field in northern Taiwan, analyzed via CODAR data in this study. However, there are still some physical mechanisms of flow paths and special flow routes that need to be studied in the future.

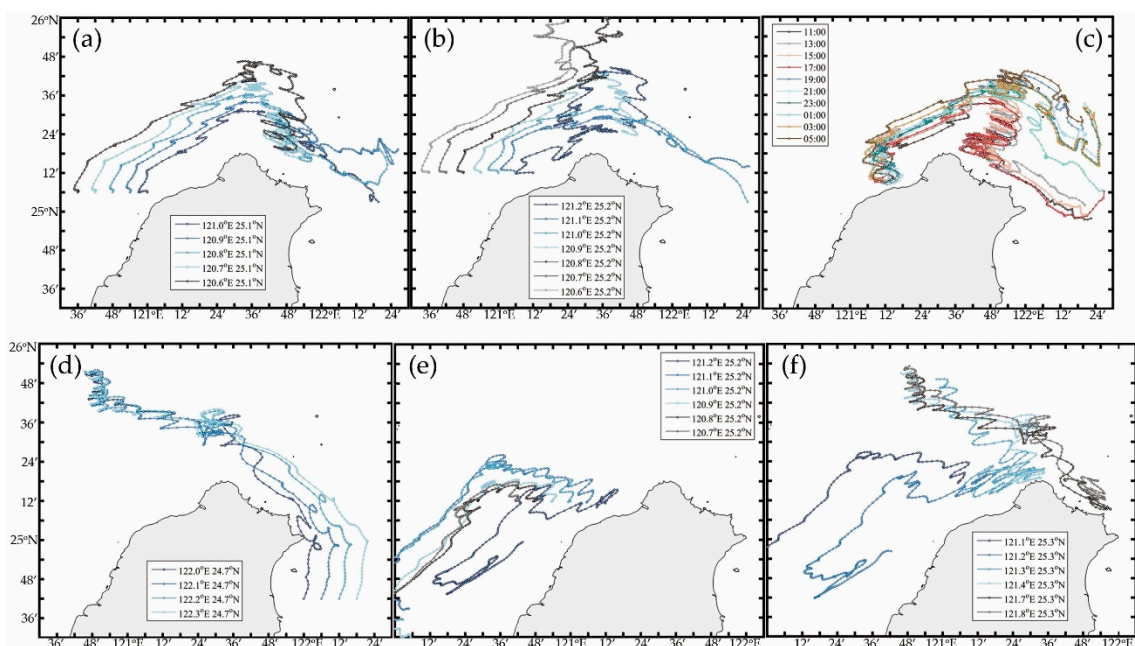


Figure 16. Simulation of virtual drifter trajectory using CODAR flow field data, simulation time of drifter on (a,b) 11:00 (UTC) 18 July, 2015, (c) from 11:00 (UTC) 8 July to 05:00 (UTC) 9 July, 2015, and (d–f) 0:00 (UTC) 19 February, 2016.

4.2. Compared with CODAR Flow Field with Buoy and Reanalysis Data

We compared the flow field from CODAR in northern Taiwan with the FGC buoy and OSCAR (ocean surface current analysis real-time) products to confirm whether they have the same flow field characteristics. The OSCAR data contain near-surface ocean current estimates derived using quasi-linear and steady flow momentum equations and combined geostrophic, Ekman, and Stommel shear dynamics. The OSCAR data from December 1992 to May 2020, with a spatial resolution of 0.33 degrees and a time resolution of 5 days, were obtained from the NASA Physical Oceanography Distributed Active Archive Center. The flow direction measured by the FGC buoy was WNW in the flood period, and the flow direction was east in the ebb period, which agrees with the CODAR observation results, except that the buoy observed faster tidal currents along the shore. The monthly average velocity obtained by OSCAR was between 0.18 to 0.25 m/s. The average velocity was 0.24 m/s in summer and 0.18 m/s in winter, which is as same as the CODAR seasonal trend, but the flow velocity is two times faster than the OSCAR dataset. The fastest velocity in summer (0.32 m/s) was in the B3 area (see Figure 3) from the CODAR results, which was close to the OSCAR dataset (0.28 m/s), and both flow directions were northeast. The fastest velocity in winter (0.21 m/s) was in the A5 area

(see Figure 3) from the CODAR results, which was also close to the OSCAR dataset (0.17 m/s), and both flow directions were northwest. Overall, the CODAR system provided high spatial (1 h) and temporal resolutions (10 km), which helped to analyze the characteristics of the flow field in northern Taiwan.

5. Conclusions

In this study, we combined historical in-situ measured ocean currents, real and virtual drifter trajectories, a CODAR ocean current observation system, GOCI chlorophyll concentration data, and Himawari-8 SST data to fully analyze the characteristics of the flow field, chlorophyll concentration changes, and the rapid change of sea surface characteristics in a short time in the north of Taiwan. Even with the statistical data of Sb-ADCP, which were only accumulated from each voyage, the historical data could still provide the flow field of the entire layer along the northern coast of Taiwan. According to the historical Sb-ADCP data from the near surface to a 70-m depth, the current state of the entire layer is mostly consistent. The trajectory obtained by the real drifter release experiment was affected by significant tidal currents, which pointed out the necessity of continuous observation for ocean currents. The hourly CODAR flow field data indicated significant changes during the ebb-flood period in the north of Taiwan. We also simulated the trajectory of a virtual drifter from the CODAR flow field dataset to classify the main seasonal characteristics of the flow field in the adjacent waters of northern Taiwan.

The ocean currents in the north of Taiwan have significant short-term tidal variations and special seasonal changes based on the CODAR flow field. They can summarize as a schematic diagram in Figure 17. The current flowed westward during the ebb period and eastward during the flood period. In summer, the flow velocity was 0.43 m/s during the ebb period and 0.26 m/s during the flood period. However, in winter, the velocity characteristics were opposite, namely, 0.27 m/s during the ebb period and 0.45 m/s during the flood period. In summer, the current on the side of the Taiwan Strait flows northward and is divided into two branches off the northwestern coast of Taiwan. One branch flows northward and the other branches along the northern coast of Taiwan at 0.15 m/s eastward into the Kuroshio region. The mainstream of the Taiwan Strait has a low concentration of chlorophyll, but the near shore could be exposed to river runoff to maintain a high concentration of chlorophyll, and it is mainly diffused within the 100-m isobath. In winter, the Kuroshio branch invades the ECS shelf, where the northern waters move westward at a velocity of 0.08 m/s. The high concentration of chlorophyll is entrained by the dilute water of the rivers along the coast of China and flows southward to the Taiwan Strait. The average chlorophyll concentration on the northwestern coast of Taiwan from November to January exceeded 2.0 mg/m^3 here. Both the real and virtual drifter trajectory experiments showed that the ocean currents in the north of Taiwan are highly unpredictable. The example cases also indicated that the chlorophyll concentration would have significant diurnal changes during the short-term within rapid current movement. In conclusion, this study has combined CODAR flow field observation technology and geosynchronous satellite monitoring to establish more complete knowledge in physical oceanography of the northern Taiwan waters to facilitate the integration of multidisciplinary research between the TS, the ECS, and the Kuroshio.

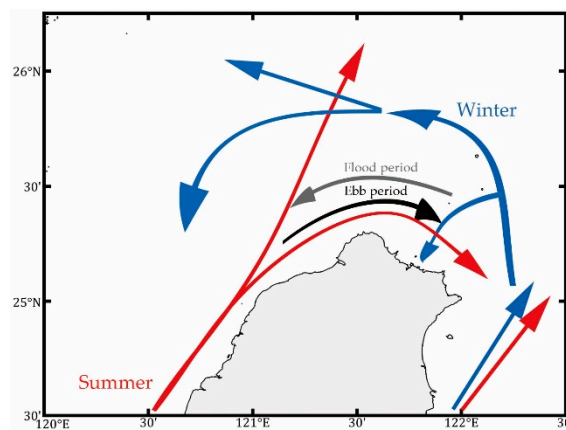


Figure 17. A schematic diagram of the main characteristics of the flow field in the north of Taiwan.

Author Contributions: Conceptualization, P.-C.H. & C.-R.H.; methodology, P.-C.H.; software, P.-C.H. and C.-Y.L.; validation, P.-C.H. & C.-R.H.; formal analysis, P.-C.H. and C.-Y.L.; investigation, P.-C.H.; resources, C.-R.H.; data curation, P.-C.H. and C.-Y.L.; writing-original draft manuscript, P.-C.H.; writing-review and editing, P.-C.H., T.-W.H., and C.-R.H.; project administration, C.-R.H.; funding acquisition, C.-R.H. All authors have read and agreed to the published version of the manuscript.

Funding: This research and the APC was funded by the Ministry of Science and Technology of Taiwan through grants MOST 108-2611-M-019-019, MOST 108-2811-M-019-506, MOST 109-2611-M-019-001, and MOST 109-2811-M-019-502.

Acknowledgments: The authors appreciate all the data use provided from each open database. The GOCI data were obtained from the NASA ocean color web (<https://oceancolor.gsfc.nasa.gov/data/goci/>); The CODAR dataset were provided by Taiwan Ocean Research Institute, National Applied Research Laboratories (<https://www.tori.narl.org.tw/ETORI/eDefault.aspx>); The drifter data were download from National Oceanic and Atmospheric Administration Atlantic Oceanographic and Meteorological Laboratory Physical Oceanography Division (<https://www.aoml.noaa.gov/phod/gdp/index.php>); The Himawari-8 SST and Chl-a data were supplied by the P-Tree System, JAXA (<http://www.eorc.jaxa.jp/ptree/>); the OSCAR ocean currents data were download from NASA PODAAC (<https://doi.org/10.5067/OSCAR-03D01>); the open historical Sb-ADCP data obtained from the Ocean Data Bank of the Ministry of Science and Technology of Taiwan (<http://www.odb.ntu.edu.tw/en/>). The buoy and tidal station data obtained from Central Weather Bureau, Taiwan (<https://www.cwb.gov.tw/eng/>).

Conflicts of Interest: The authors declare no conflict of interest.

Appendix A

Detailed flow observation data at 15 locations in northern Taiwan.

Table A1. Seasonal flow field data from Sb-ADCP data (Figure 3). S represents the flow speed (m/s) and D represents the flow direction (sixteen bearings).

Spring (March to May)														
	D	S		D	S		D	S		D	S		D	S
A1	N	0.33	A2	N	0.17	A3	ESE	0.29	A4	NW	0.29	A5	NE	0.04
B1	NNE	0.35	B2	NNE	0.18	B3	ESE	0.12	B4	SE	0.20	B5	SE	0.18
C1	NE	0.63	C2	ENE	0.14	C3	N	0.05	C4	SE	0.09	C5	E	0.15
Summer (Jun to August)														
	D	S		D	S		D	S		D	S		D	S
A1	NNE	0.29	A2	NE	0.45	A3	ENE	0.31	A4	S	0.08	A5	SSW	0.18
B1	NE	0.63	B2	NE	0.33	B3	N	0.03	B4	SE	0.08	B5	S	0.21
C1	NE	0.80	C2	ENE	0.21	C3	NNE	0.15	C4	SSE	0.15	C5	SE	0.22
Fall (September to November)														
	D	S		D	S		D	S		D	S		D	S
A1	NE	0.38	A2	NE	0.25	A3	WNW	0.31	A4	S	0.13	A5	ENE	0.07
B1	NNW	0.26	B2	W	0.18	B3	SSW	0.15	B4	WNW	0.33	B5	E	0.05
C1	NNE	0.26	C2	SSW	0.02	C3	N	0.09	C4	SE	0.07	C5	SE	0.15
Winter (December to February)														
	D	S		D	S		D	S		D	S		D	S
A1	NE	0.12	A2	E	0.44	A3	NE	0.17	A4	NW	0.70	A5	N	0.34
B1	W	0.46	B2	E	0.45	B3	ENE	0.42	B4	NNW	0.38	B5	NW	0.50
C1	NNW	0.14	C2	SW	0.19	C3	NE	0.14	C4	SSE	0.07	C5	NNW	0.07

Table A2. Seasonal flow field data from the CODAR data (Figure 8). S represents the flow speed (m/s) and D represents the flow direction (sixteen bearings).

Spring (March to May)														
	D	S		D	S		D	S		D	S		D	S
A1	N	0.17	A2	NNE	0.13	A3	NE	0.04	A4	ENE	0.07	A5	NE	0.09
B1	NNE	0.20	B2	NE	0.16	B3	ENE	0.05	B4	ESE	0.09	B5	E	0.09
C1	NNE	0.20	C2	NNE	0.09	C3	NE	0.06	C4	SSE	0.08	C5	ESE	0.11
Summer (Jun to September)														
	D	S		D	S		D	S		D	S		D	S
A1	NNE	0.29	A2	NE	0.22	A3	NE	0.09	A4	E	0.08	A5	ESE	0.12
B1	NE	0.32	B2	NE	0.23	B3	ENE	0.07	B4	SE	0.08	B5	SE	0.11
C1	NE	0.27	C2	NE	0.12	C3	NE	0.04	C4	S	0.06	C5	SE	0.14
Fall (October and November)														
	D	S		D	S		D	S		D	S		D	S
A1	WNW	0.09	A2	WSW	0.04	A3	SSW	0.06	A4	NNE	0.02	A5	NE	0.04
B1	WNW	0.07	B2	WSW	0.01	B3	SSE	0.04	B4	SE	0.06	B5	ESE	0.05
C1	NW	0.09	C2	W	0.06	C3	NNE	0.01	C4	SSW	0.11	C5	SE	0.09
Winter (December to February)														
	D	S		D	S		D	S		D	S		D	S
A1	W	0.06	A2	W	0.05	A3	W	0.05	A4	WNW	0.16	A5	NW	0.21
B1	WNW	0.04	B2	WSW	0.02	B3	W	0.01	B4	WNW	0.12	B5	NW	0.17
C1	WNW	0.05	C2	WSW	0.04	C3	NNW	0.03	C4	SW	0.09	C5	WNW	0.05

Table A3. Flow data during the ebb period from the CODAR data (Figure 9). S represent the flow speed (m/s) and D represents the flow direction (sixteen bearings).

Spring (March to May)														
	D	S		D	S		D	S		D	S		D	S
A1	ENE	0.31	A2	ENE	0.32	A3	E	0.26	A4	E	0.37	A5	E	0.38
B1	ENE	0.39	B2	ENE	0.47	B3	E	0.31	B4	ESE	0.43	B5	ESE	0.40
C1	NE	0.43	C2	ENE	0.42	C3	ENE	0.40	C4	ESE	0.38	C5	ESE	0.36
Summer (Jun to September)														
	D	S		D	S		D	S		D	S		D	S
A1	ENE	0.48	A2	ENE	0.43	A3	ENE	0.28	A4	ESE	0.38	A5	ESE	0.47
B1	NE	0.55	B2	ENE	0.58	B3	ENE	0.31	B4	ESE	0.44	B5	ESE	0.47
C1	NE	0.51	C2	ENE	0.48	C3	ENE	0.37	C4	ESE	0.35	C5	ESE	0.39
Fall (Oct and November)														
	D	S		D	S		D	S		D	S		D	S
A1	E	0.19	A2	E	0.31	A3	ESE	0.30	A4	E	0.34	A5	ESE	0.40
B1	ENE	0.24	B2	E	0.43	B3	E	0.34	B4	ESE	0.44	B5	ESE	0.44
C1	ENE	0.25	C2	ENE	0.36	C3	ENE	0.39	C4	ESE	0.35	C5	SE	0.36
Winter (December to February)														
	D	S		D	S		D	S		D	S		D	S
A1	E	0.21	A2	E	0.27	A3	E	0.25	A4	E	0.23	A5	E	0.20
B1	ENE	0.25	B2	E	0.38	B3	E	0.31	B4	E	0.25	B5	E	0.21
C1	ENE	0.26	C2	ENE	0.35	C3	ENE	0.35	C4	ESE	0.30	C5	ESE	0.24

Table A4. Flow data during the flood period from the CODAR data (Figure 10). S represents the flow speed (m/s) and D represents the flow direction (sixteen bearings).

Spring (March to May)														
	D	S		D	S		D	S		D	S		D	S
A1	WNW	0.30	A2	WNW	0.26	A3	WNW	0.24	A4	WNW	0.32	A5	NW	0.38
B1	WNW	0.25	B2	W	0.29	B3	W	0.26	B4	WNW	0.33	B5	WNW	0.31
C1	WNW	0.20	C2	W	0.35	C3	WSW	0.36	C4	WSW	0.32	C5	WNW	0.20
Summer (Jun to September)														
	D	S		D	S		D	S		D	S		D	S
A1	NNW	0.27	A2	NW	0.21	A3	WNW	0.18	A4	WNW	0.27	A5	WNW	0.29
B1	NNW	0.22	B2	WNW	0.26	B3	W	0.21	B4	W	0.36	B5	WNW	0.33
C1	NW	0.17	C2	WSW	0.32	C3	WSW	0.34	C4	W	0.36	C5	W	0.17
Fall (October and November)														
	D	S		D	S		D	S		D	S		D	S
A1	W	0.40	A2	W	0.44	A3	W	0.40	A4	WNW	0.38	A5	WNW	0.41
B1	W	0.37	B2	W	0.51	B3	W	0.36	B4	W	0.41	B5	WNW	0.39
C1	W	0.40	C2	WSW	0.54	C3	WSW	0.43	C4	W	0.39	C5	WNW	0.23
Winter (December to February)														
	D	S		D	S		D	S		D	S		D	S
A1	W	0.36	A2	W	0.41	A3	W	0.40	A4	WNW	0.59	A5	WNW	0.63
B1	W	0.36	B2	WSW	0.49	B3	W	0.36	B4	WNW	0.52	B5	WNW	0.57
C1	WSW	0.38	C2	WSW	0.49	C3	WSW	0.42	C4	W	0.43	C5	WNW	0.38

References

1. Jan, S.; Wang, J.; Chern, C.S.; Chao, S.Y. Seasonal variation of the circulation in the Taiwan Strait. *J. Mar. Syst.* **2002**, *35*, 249–268. [[CrossRef](#)]

2. Jan, S.; Sheu, D.D.; Kuo, H.M. Water mass and throughflow transport variability in the Taiwan Strait. *J. Geophys. Res. Oceans* **2006**, *111*, C12012. [[CrossRef](#)]
3. Tseng, H.C.; You, W.L.; Huang, W.; Chung, C.C.; Tsai, A.Y.; Chen, T.Y.; Lan, K.W.; Gong, G.C. Seasonal variations of marine environment and primary production in the Taiwan Strait. *Front. Mar. Sci.* **2020**, *7*, 38. [[CrossRef](#)]
4. Hsieh, C.H.; Chen, C.S.; Chiu, T.S. Composition and abundance of copepods and ichthyoplankton in Taiwan Strait (western North Pacific) are influenced by seasonal monsoons. *Mar. Freshw. Res.* **2005**, *56*, 153–161. [[CrossRef](#)]
5. Hwang, J.S.; Souissi, S.; Tseng, L.C.; Seuront, L.; Schmitt, F.G.; Fang, L.S.; Peng, S.H.; Wu, C.H.; Hsiao, S.H.; Twan, W.H.; et al. A 5-year study of the influence of the northeast and southwest monsoons on copepod assemblages in the boundary coastal waters between the East China Sea and the Taiwan Strait. *J. Plankton Res.* **2006**, *28*, 943–958. [[CrossRef](#)]
6. Chen, H.Y.; Chen, Y.L.L. Quantity and quality of summer surface net zooplankton in the Kuroshio current-induced upwelling northeast of Taiwan. *Terr. Atmos. Ocean. Sci.* **1992**, *3*, 321–334. [[CrossRef](#)]
7. Su, W.C.; Lo, W.T.; Liu, D.C.; Wu, L.J.; Hsieh, H.Y. Larval fish assemblages in the Kuroshio waters east of Taiwan during two distinct monsoon seasons. *Bull. Mar. Sci.* **2011**, *87*, 13–29. [[CrossRef](#)]
8. Naimullah, M.; Lan, K.W.; Liao, C.H.; Hsiao, P.Y.; Liang, Y.R.; Chiu, T.C. Association of environmental factors in the taiwan strait with distributions and habitat characteristics of three swimming crabs. *Remote Sens.* **2020**, *12*, 2231. [[CrossRef](#)]
9. Choi, J.; Park, Y.G.; Kim, W.; Kim, Y.H. Characterization of submesoscale turbulence in the east/japan sea using geostationary ocean color satellite images. *Geophys. Res. Lett.* **2019**, *46*, 8214–8223. [[CrossRef](#)]
10. Higa, H.; Sugahara, S.; Salem, S.I.; Nakamura, Y.; Suzuki, T. An estimation method for blue tide distribution in Tokyo Bay based on sulfur concentrations using Geostationary Ocean Color Imager (GOCI). *Estuar. Coast. Shelf Sci.* **2020**, *235*, 106615. [[CrossRef](#)]
11. Park, J.E.; Park, K.A.; Kang, C.K.; Park, Y.J. Short-term response of chlorophyll-a concentration to change in sea surface wind field over mesoscale eddy. *Estuar. Coasts* **2020**, *43*, 646–660. [[CrossRef](#)]
12. Jan, S.; Chen, C.C.; Tsai, Y.L.; Yang, Y.J.; Wang, J.; Chern, C.S.; Gawarkiewicz, G.; Lien, R.C.; Centurioni, L.; Kuo, J.Y. Mean structure and variability of the cold dome northeast of Taiwan. *Oceanography* **2011**, *24*, 100–109. [[CrossRef](#)]
13. Hsu, P.C.; Zheng, Q.; Lu, C.Y.; Cheng, K.H.; Lee, H.J.; Ho, C.R. Interaction of coastal countercurrent in I-Lan Bay with the Kuroshio northeast of Taiwan. *Cont. Shelf Res.* **2018**, *171*, 30–41. [[CrossRef](#)]
14. Yin, Y.; Liu, Z.; Hu, P.; Hou, Y.; Lu, J.; He, Y. Impact of mesoscale eddies on the southwestward countercurrent northeast of Taiwan revealed by ADCP mooring observations. *Cont. Shelf Res.* **2020**, *195*, 104063. [[CrossRef](#)]
15. He, Y.; Hu, P.; Yin, Y.; Liu, Z.; Liu, Y.; Hou, Y.; Zhang, Y. Vertical migration of the along-slope counter-flow and its relation with the Kuroshio intrusion off northeastern Taiwan. *Remote Sens.* **2019**, *11*, 2624. [[CrossRef](#)]
16. Shen, Y.T.; Lai, J.W.; Leu, L.G.; Lu, Y.C.; Chen, J.M.; Shao, H.J.; Chen, H.W.; Chang, K.T.; Terng, C.T.; Chang, Y.C.; et al. Applications of ocean currents data from high-frequency radars and current profilers to search and rescue missions around Taiwan. *J. Oper. Oceanogr.* **2019**, *12* (Suppl. 2), S126–S136. [[CrossRef](#)]
17. Hsu, P.C.; Lee, H.J.; Zheng, Q.; Lai, J.W.; Su, F.C.; Ho, C.R. Tide-induced periodic sea surface temperature drops in the coral reef area of Nanwan Bay, southern Taiwan. *J. Geophys. Res. Oceans* **2020**, *125*, e2019JC015226. [[CrossRef](#)]
18. NASA Goddard Space Flight Center, Ocean Ecology Laboratory, Ocean Biology Processing Group. *Geostationary Ocean Color Imager (GOCI) Ocean Color Data*; 2014 Reprocessing; NASA OB.DAAC: Greenbelt, MD, USA, 2014. Available online: <https://oceancolor.gsfc.nasa.gov/data/10.5067/COMS/GOCI/L2/OC/2014> (accessed on 23 June 2020).
19. Hsu, P.C.; Ho, C.Y.; Lee, H.J.; Lu, C.Y.; Ho, C.R. Temporal variation and spatial structure of the Kuroshio-induced submesoscale island vortices observed from GCOM-C and Himawari-8 data. *Remote Sens.* **2020**, *12*, 883. [[CrossRef](#)]

20. Elipot, S.; Lumpkin, R.; Perez, R.C.; Lilly, J.M.; Early, J.J.; Sykulski, A.M. A global surface drifter data set at hourly resolution. *J. Geophys. Res. Oceans* **2016**, *121*, 2937–2966. [[CrossRef](#)]
21. Chen, C.T.A. Distributions of nutrients in the East China Sea and the South China Sea connection. *J. Oceanogr.* **2008**, *64*, 737–751. [[CrossRef](#)]



© 2020 by the authors. Licensee MDPI, Basel, Switzerland. This article is an open access article distributed under the terms and conditions of the Creative Commons Attribution (CC BY) license (<http://creativecommons.org/licenses/by/4.0/>).